S1293-2558(05)00072-5/FLA AID:2505 Vol.●●●(●●●)
SSSCIE:m5 v 1.36 Prn:8/04/2005; 12:11

ssscie2505

[DTD5] P.1 (1-10)
by:Vik p. 1

Available online at www.sciencedirect.com
SCIENCE DIRECT®

Solid State Sciences ●●● (●●●●) ●●●–●●●

www.elsevier.com/locate/ssscie

Inhibition of Nd magnetic order in $NdFe_{1-x}Co_xO_3$ ($x \leqslant 0.5$)

F. Bartolomé, J. Bartolomé *

ICMA—Departamento de Física de la Materia Condensada, CSIC—Universidad de Zaragoza, 50009 Zaragoza, Spain

Received 4 November 2004; accepted 9 November 2004

Abstract

The low-temperature specific heat of the $NdFe_{1-x}Co_xO_3$ ($x = 0$, 0.03, 0.1, 0.25, and 0.5) solid solutions has been measured in order to study the magnetic ordering of the Nd sublattice as a function of the Co content. The experimental results show the inhibition of the Nd magnetic ordering for $x \geqslant 0.1$. Bertaut's theory of spin configurations for ionic structures is used to propose a simple mean-field model which is able to explain the main features of the low-temperature heat capacity of $NdFe_{1-x}Co_xO_3$ for $x = 0$, 0.03 and 0.1 in terms of the ratio between the Nd–Nd and Fe–Nd interactions. In order to properly explain the specific heat curves we find satisfactory to include a distribution of internal fields acting on the Nd^{3+} ions. Indeed, low-spin Co ions in $NdFe_{1-x}Co_xO_3$ are equivalent to magnetic vacancies and the Nd atoms are polarized additionally by an internal field caused by the Fe–Nd isotropic interaction between the non compensated Fe moments and the Nd.

PACS: 75.30.Et; 75.40.Cx; 65.40.+g

Keywords: Perovskites; Orthoferrites; Rare-earth oxides; Magnetic order; Magnetic vacancies; Low-temperature physics; Specific-heat

1. Introduction

Rare-earth oxide compounds with perovskite structure have been receiving renewed attention during the last decade in connection with the discovery of high-T_c superconductivity and colossal magnetoresistance. These compounds, with a rather simple structure provide, however, a rich variety of electronic and magnetic phenomena depending on the atoms involved, the interatomic distances and the bonding strength.

In particular, RMO_3 are model systems to investigate the magnetic interactions between the rare earth (R) and 3*d* or 4*d* metal ions (M). In general, those interactions follow the hierarchy of M–M, M–R and R–R in descending strength. The $NdMO_3$ family has a wide range of magnetic and non-magnetic M substitutions with the same structure (space group D_{16}^{2h}). The Nd^{3+} ion occupies low-symmetry position, and its $^4I_{9/2}$ ground multiplet is fully split into five Kramers doublets by the C_s-*m* low-symmetry crystal field. In the range of temperatures we are dealing with ($T < 10$ K) only the ground doublet is populated, and a description within an effective spin $s = 1/2$ is satisfactory. It has been shown [1–3] that when the $H_{\mathrm{Nd–Nd}}$ exchange interaction is isolated, i.e., M is a diamagnetic ion such as Ga, Sc, In or Co, the Nd sublattice orders at about $T \sim 1$ K. This gives rise to a lambda anomaly with the corresponding anomalous entropy $S = \ln 2$. In particular the compound $NdCoO_3$ has a long range order transition at $T_N = 1.20(1)$ K from paramagnetic to antiferromagnetic c_z (Γ_1) configuration. In this compound, which we shall deal with later in this paper, the Co^{3+} atoms are in a diamagnetic state at these temperatures [4,5].

The introduction of a magnetic 3*d* transition metal, such as Fe, Ni or Cr, leads to the magnetic ordering of the M sublattice at T_N, which ranges from ~700 K for $NdFeO_3$ to ~200 K for $NdCrO_3$ and $NdNiO_3$.

Below T_N, the M–Nd exchange interaction can be separated into isotropic and anisotropic components. In these highly symmetric antiferromagnetic compounds the result-

* Corresponding author. Tel.: +34 976761218; Fax: +34 976761229.
E-mail addresses: barto@unizar.es (J. Bartolomé), bartolom@unizar.es (F. Bartolomé).

1293-2558/$ – see front matter © 2005 Published by Elsevier SAS.
doi:10.1016/j.solidstatesciences.2004.11.016

S1293-2558(05)00072-5/FLA AID:2505 Vol.●●●(●●●)
SSSCIE:m5 v 1.36 Prn:8/04/2005; 12:11
ssscie2505
[DTD5] P.2 (1-10)
by:Vik p. 2

ing isotropic exchange is cancelled out by compensation of the contributions due to antiparallel moments. However, the compensation of the anisotropic exchange is not complete, and the net effect on the Nd^{3+} moment is the appearance of an internal field $H_{M\text{–}Nd}$ that splits the Nd ground state due to the Zeeman effect. As a result, it polarizes the Nd sublattice, thus reducing the magnetic entropy available for cooperative ordering. Depending on the strength of $H_{M\text{–}Nd}$, cooperative order of the Nd sublattice appears in some cases at a lower temperature T_{N2}, as in $NdFeO_3$ [6], or $NdNiO_3$ [7] while it is fully inhibited in others, as in $NdCrO_3$ [8] or $NdMnO_3$ [9].

A landmark on the understanding of complex magnetic systems was established by E.F. Bertaut in his 1963 well known review paper [10]. Indeed, the definition of a proper bases of generalized Néel vectors for a given system (the "Bertaut's modes") allows, quoting Ref. [10] "*to infer magnetic properties from knowledge of the symmetry of the structure and vice versa*". Using the Bertaut's modes, we proposed a simple mean-field model which in terms of the ratio between $H_{Fe\text{–}Nd}$ and $H_{Nd\text{–}Nd}$ was able to explain the main features of the low-temperature heat capacity of $NdMO_3$ systems [2,6,7]: the λ peak at T_{N2} and the Schottky maximum due to Zeeman splitting. The internal field $H_{M\text{–}Nd}$ polarizes the Nd moments in a magnetic structure having the same symmetry (i.e., belongs to the same irreducible representation) than the M magnetic order established at T_N, as clearly seen by neutron diffraction. When the Van Vleck susceptibility $\chi_{V.V.}$ is introduced, our model predicts as well the temperature dependence of the magnetic neutron elastic peaks, which for example, compares satisfactorily with the experimental data for $NdFeO_3$ [6]. As the experimental specific heat evidences a true phase transition for some systems at $T_{N2} \sim 1$ K, the Nd–Nd interaction must favor a magnetic arrangement belonging to a different irreducible representation of the magnetic group than the M sublattice.

In $NdFeO_3$ the interaction ratio $H_{Fe\text{–}Nd}/H_{Nd\text{–}Nd}$ is found just below the critical value which would inhibit Nd cooperative order. As a result the Nd long range sublattice ordering is not inhibited. Indeed, it gives rise to a small anomaly at $T_{N2} = 1.05(1)$ K which can be discerned in the low temperature side of a Schottky anomaly, the latter with a maximum at $T_{max} = 2.35(5)$ K [11].

The substitution of Fe by non-magnetic Co in $NdFe_{1-x}Co_xO_3$ can be considered as the introduction of a magnetic vacancy in the Fe sublattice. Its presence in the nearest neighborhood of a rare earth ion leads to the breakdown of the compensation of the isotropic component of $H_{Fe\text{–}Nd}$. As a result of this non-compensation, an isotropic exchange field acts on the rare earth and the Fe sublattices. Indeed, a small concentration of vacancies has an important effect on the magnetic properties of rare-earth orthoferrites: in diluted $DyFe_{1-x}Al_xO_3$, the Morin phase transition temperature increases [12]. The net effect on the magnetic ordering of the rare earth depends in detail of the competition between the crystal electric field and the exchange field. In $TbFe_{1-x}Al_xO_3$, the reorientation transition temperature from a configuration belonging to Γ_4 to another belonging to Γ_2 decreases in temperature [13] while the Tb long-range order is inhibited. Even in $HoFe_{1-x}Al_xO_3$ a new transition, to Γ_1 configuration is induced by vacancies [14,15].

So, the substitution of Fe by non-magnetic Co is an excellent test case to study the modification of the effect of vacancies on the magnetic ordering of the Nd sublattice, so far never studied. The vacancies modify the $H_{Fe\text{–}Nd}$ interaction, and therefore this opens the possibility to evaluate the ability of the model to explain the induced effects. The Fe sublattice is known to order antiferromagnetically at $T_N = 687$ K [16], so, the magnetic dilution of the Fe sublattice provokes the lowering of T_N till the quenching of magnetic ordering for $x \geqslant 0.65$, the percolation limit. This fact creates two different scenarios in the study of the Nd sublattice. For low x concentrations the Fe sublattice is ordered but contains randomly distributed magnetic vacancies, while for high x values the Fe moments are paramagnetically disordered, and decorate randomly the Nd lattice.

In this paper we shall study the low Co content region of $NdFe_{1-x}Co_xO_3$, in detail. The scheme of the paper is as follows; in Sections 2 and 3 the experimental details and results are given, in Section 4 the mean field model is introduced and predictions are compared with the experiment. In Section 5 we discuss the validity of the model and Section 6 are our conclusions.

2. Experimental details

The specific heat measurements in the range $0.3\ \text{K} < T < 6\ \text{K}$ were performed using a fully automated quasi-adiabatic calorimeter [3] refrigerated by adiabatic demagnetization of a paramagnetic salt (CPA), using heat pulse technique and germanium thermometry in the whole temperature range. The absolute accuracy of the instrument has been estimated to be about 1%. The calorimetric data measured for $x = 0$ and 0.5 between 4 K and 275 K, were obtained in a commercial Sinku-Riko AC-calorimeter. The relative values obtained by this technique have an accuracy of 0.1%. They were scaled to the absolute values measured at low-temperature.

$NdFe_{1-x}Co_xO_3$ powder samples ($x = 0$, 0.03, 0.1, 0.25, 0.5 and 1) were obtained by using a ceramic procedure. A stoichiometric mixture of the binary oxides in the appropriate proportions to achieve the desired solid solutions was calcined in air at 1000 °C for 2 days with intermediate grindings. The resulting powder was pressed to 5 kbar into pellets and sintered in air at 1300 °C for 6 h. For the low temperature experiments, about 0.5 g of sample were mixed with Apiezon N grease to achieve a good thermal contact even at the lowest temperatures between the sample and the calorimetric set (heater and thermometer).

S1293-2558(05)00072-5/FLA AID:2505 Vol.●●●(●●●)
SSSCIE:m5 v 1.36 Prn:8/04/2005; 12:11
ssscie2505
[DTD5] P.3 (1-10)
by:Vik p. 3

3. Experimental results

In Fig. 1, we show the specific heat of the $NdFe_{1-x}Co_xO_3$ series measured below 6 K, except for $x = 1$ ($NdCoO_3$) which is shown for comparison, and only below 4 K. The specific heat of $NdFeO_3$ ($x = 0$), shown in the left upper panel of Fig. 1, features a well known Schottky-like anomaly [11], with a maximum at $T = 2.35$ K (about 7% lower than the ideal doublet Schottky curve), as well as a small sharp peak at $T_{N2} = 1.05$ K already mentioned in Section 1, thus proving the on-set of Nd long range order. The same general features are found in the specific heat for $x = 0.03$. However the Nd critical temperature decreases to $T_{N2} = 0.72$ K, slightly increasing the temperature of the Schottky maximum (from $T = 2.35$ K to $T = 2.6$ K) as well as its height, which is nearer to the ideal Schottky value. For $x = 0.1$ only, the small λ peak on the low-temperature side has already disappeared, and the Schottky maximum appears at $T = 2.9$ K.

Thus, the dilution of Fe with diamagnetic Co destroys the cooperative ordering of Nd at low-temperature for Co contents as low as a few percent. This is accompanied with a slight but clear trend of shifting the Schottky maximum to higher temperatures for increasing x, corresponding to an enhancement of the Zeeman splitting of the Nd ground doublet from ~6 K ($x = 0$) to ~7 K ($x = 0.1$). Within the theoretical frame given for $NdFeO_3$ in Section 1, those trends are indicative of the increase of the internal field acting on the Nd sublattice from $x = 0$ to $x = 0.1$. Our experimental results point out that the Co dilution drives the ratio of interactions $r = H_{Fe-Nd}/H_{Nd-Nd}$ above the critical limit, thus inhibiting Nd cooperative order.

The specific heat curves for $x = 0.25$ and $x = 0.5$ are similar to the $x = 0.1$ one. However, the two trends observed in the range $0 \leqslant x \leqslant 0.1$ are reversed on the $0.1 \leqslant x \leqslant 0.5$ region: the temperature of the maximum C_p stabilizes and starts decreasing, while the height of the Schottky-like hump decreases when x increases. Its shape is strongly distorted with the Co concentration, completely loosing the characteristic two-level Schottky shape. This may be indicative of a broad distribution of Zeeman splittings of Nd^{3+} ions. Indeed, in first approximation, each Nd ion is affected by 8 nearest Fe or Co neighbors, and the strength of the magnetic interaction may vary depending on the number of Co ions and the magnetic configuration of the Fe ones. We will show in Section 4 how to rationalize this dependence in order to explain the specific heat for $x = 0.5$.

Finally, $NdCoO_3$ ($x = 1$), shown for comparison, presents the characteristic λ peak of antiferromagnetic ordering at $T = 1.2$ K, Nd being the only magnetic species, similarly to what was found in $NdGaO_3$ [1,17], $NdScO_3$, and $NdInO_3$ [3]. The critical temperature of Nd for $x = 0$ and $x = 1$ is approximately constant, as shown in Table 1.

The results shown in Fig. 1 can be summarized in a phase diagram as presented in Fig. 2. The grey area, marked "**AF**" corresponds to cooperative order of both, Nd and Fe sublattices. The white area falls within the percolative region for the Fe sublattice, as its ordering is expected to disappear only above a substitution rate $x > (1 - p_c) = 0.693$, where $p_c = 0.307$ is the percolation limit for a Heisenberg simple cubic two sublattice antiferromagnet, as applicable for a $S = 5/2$ system [18]. Thus, in the white region of

Table 1
Relevant thermodynamic data obtained from the specific heat measurements shown in Fig. 1

x	T_{N2} (K)	T_{max} (K)	C_{max} (R)	S_c (R)	S_{Sch} (K)	$S\,(R/\ln 2)$
0	1.05(1)	2.20(5)	0.388(3)	0.068	0.60	0.98
0.03	0.72(2)	2.6(1)	0.396(4)	0.028	0.67	1.01
0.1	–	2.95(5)	0.392(2)	–	0.69	1.0
0.25	–	3.00(5)	0.380(2)	–	0.68	0.98
0.5	–	2.8(2)	0.317(5)	–	0.73	1.05
1	1.20	–	–	0.39	–	0.99

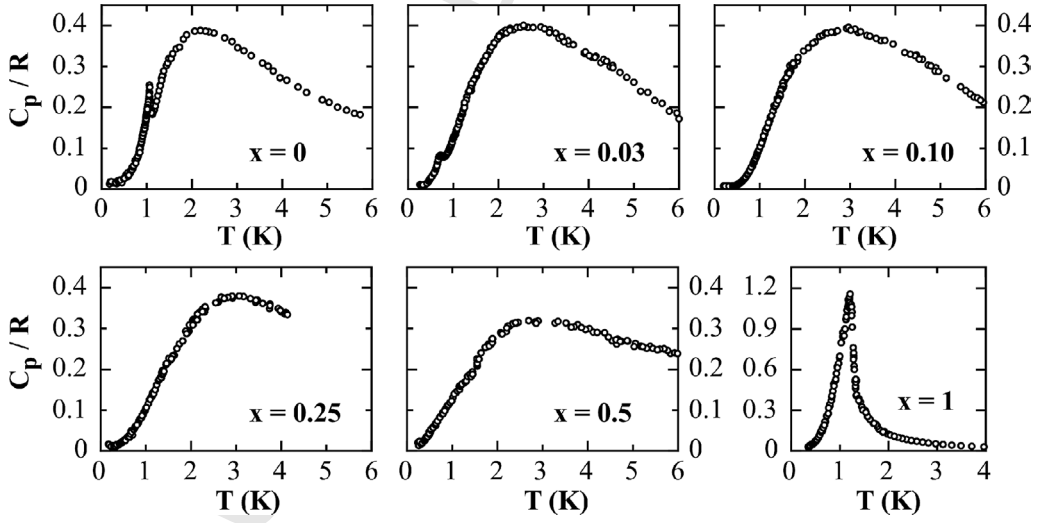

Fig. 1. Specific heat of the $NdFe_{1-x}Co_xO_3$ system. Note that the temperature scales are common for all the figures, as well as the vertical ones except for that corresponding to $x = 1$.

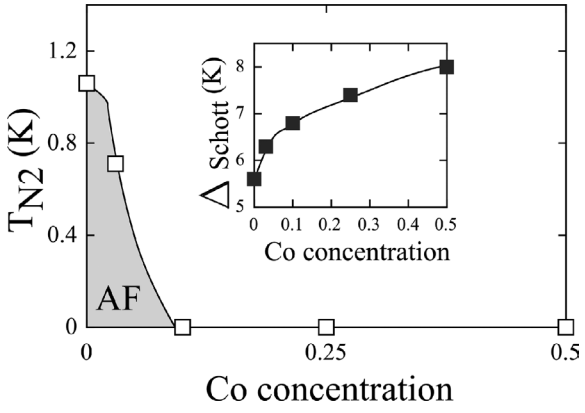

Fig. 2. Low-temperature phase diagram of $NdFe_{1-x}Co_xO_3$ for $x \leqslant 0.5$ after the experimental results. The grey area corresponds to cooperative order of both, Nd and Fe sublattices, while over the white area only Fe is ordered, Nd being polarized by $H_{\text{Fe–Nd}}$ interaction.

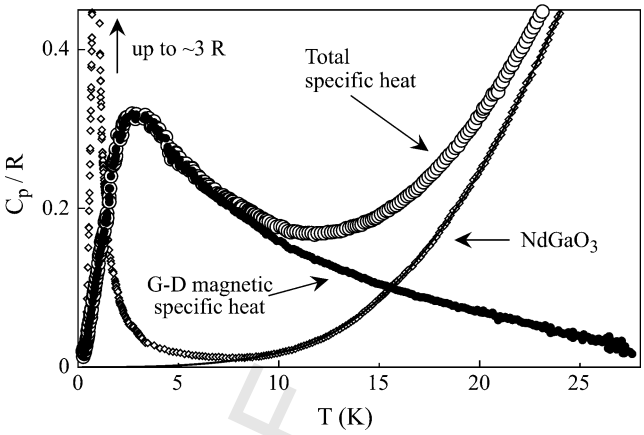

Fig. 3. The ground-doublet magnetic specific heat (•) of the $NdFe_{1-x}Co_xO_3$ systems has been obtained by subtraction of the *base-line* (full line) from the experimental data (○). The $NdGaO_3$ specific heat is also shown (◇).

Fig. 2, only Fe is ordered, while Nd is being polarized by the $H_{\text{Fe–Nd}}$ interaction. The degree of polarization can be quantified by the average splitting of the Nd^{3+} ground doublet, Δ_{Schott}, shown as a function of Co concentration in the inset of Fig. 2. The continuous increase of Δ_{Schott} upon Co concentration evidences the increase of the internal average field acting on the Nd sublattice from $x = 0$ to $x = 0.5$. The detailed procedure to derive Δ_{Schott} from the specific heat data will be detailed in Section 5.

In order to obtain the magnetic specific heat of $NdFe_{1-x}Co_xO_3$, the lattice contribution affecting the curves shown in Fig. 1 has to be evaluated and subtracted, if necessary. Although it has been shown that both the lattice specific heat and the Schottky contributions from excited doublets can be neglected below ~5 K in $NdMO_3$ systems, we have to extend the calorimetric study at higher temperatures for some members of the $NdFe_{1-x}Co_xO_3$ series, namely $x = 0.5$. Moreover, our aim is to compare the experimental curves with the results of a $S = 1/2$ model, and to do so any sizeable contribution from excited doublets overlapped to the ground doublet one, if present, should be also taken into account. The specific heat analysis performed on our data is exemplified in Fig. 3.

In $NdMO_3$ pure systems with diamagnetic M atoms [3], and in particular in $NdGaO_3$ [1,17], the high temperature side of the λ peak is very well described by a T^{-2} law and thus, can be calculated up to any temperature. Both the crystal structure and the $^4I_{9/2}$ crystal field splitting are very similar along the whole series of orthorhombic $NdMO_3$ compounds. Thus, by subtracting from the experimental specific heat of $NdGaO_3$ the well-known magnetic contribution of the ground-doublet, we get a curve (full line in Fig. 3) which consists of a lattice specific heat plus a Schottky contribution from excited doublets providing the required *base-line* for the $NdFe_{1-x}Co_xO_3$ system. The soundness of the procedure is assured by the fact that the entropy of the removed specific heat in $NdGaO_3$ equals $R \ln 2$ within the experimental accuracy [1]. Fig. 3 shows the $NdFe_{0.5}Co_{0.5}O_3$ specific heat data (○), together with the *base-line* and the result of the subtraction (•), labelled "G-D magnetic specific heat". The specific heat of $NdGaO_3$ is also shown (◇), to evidence the procedure followed to obtain the *base-line*. It is worth to note that in $NdFe_{1-x}Co_xO_3$, the specific heat from spurious contributions below ~5 K is negligible in comparison to the magnetic one. The data shown in Fig. 1 are not appreciably modified by this subtraction procedure.

In the low-temperature side, it has been shown that the hyperfine contribution to the heat capacity in $NdMO_3$ systems is negligible above ~250 mK [19] in comparison with the magnetic specific heat of interest here, with the only exception of $NdCrO_3$ where the hyperfine contribution is observable below $T = 1$ K. Thus, we will neglect this contribution, even if a tiny up-turn can be appreciated at the lowest temperatures in the specific heat of some samples.

4. Mean field model

$NdFeO_3$ and $NdCoO_3$ have an orthorhombically distorted perovskite structure, space group D_{16}^{2h} (*Pbnm*), with four formula units per elementary cell, schematically shown in Fig. 4.

The magnetic configurations are described in terms of eigenstates (Bertaut's modes) of linear combinations of spin operators for different 3*d* metal or rare-earth sites, whose Cartesian components transform as one of the eight one-dimensional irreducible representations of the reduced space group. These linear combinations are:

$$\begin{aligned}
\hat{\mathbf{f}}_{M,R} &= \hat{\mathbf{s}}_{1,5} + \hat{\mathbf{s}}_{2,6} + \hat{\mathbf{s}}_{3,7} + \hat{\mathbf{s}}_{4,8},\\
\hat{\mathbf{g}}_{M,R} &= \hat{\mathbf{s}}_{1,5} - \hat{\mathbf{s}}_{2,6} + \hat{\mathbf{s}}_{3,7} - \hat{\mathbf{s}}_{4,8},\\
\hat{\mathbf{c}}_{M,R} &= \hat{\mathbf{s}}_{1,5} + \hat{\mathbf{s}}_{2,6} - \hat{\mathbf{s}}_{3,7} - \hat{\mathbf{s}}_{4,8},\\
\hat{\mathbf{a}}_{M,R} &= \hat{\mathbf{s}}_{1,5} - \hat{\mathbf{s}}_{2,6} - \hat{\mathbf{s}}_{3,7} + \hat{\mathbf{s}}_{4,8}
\end{aligned} \tag{1}$$

where $\hat{\mathbf{s}}_{M,R}$ are the electronic spins of the 3*d* (Nd) ion of the structure schematized in Fig. 4. Following the usual no-

S1293-2558(05)00072-5/FLA AID:2505 Vol.●●●(●●●)
SSSCIE:m5 v 1.36 Prn:8/04/2005; 12:11
ssscie2505
[DTD5] P.5 (1-10)
by:Vik p. 5

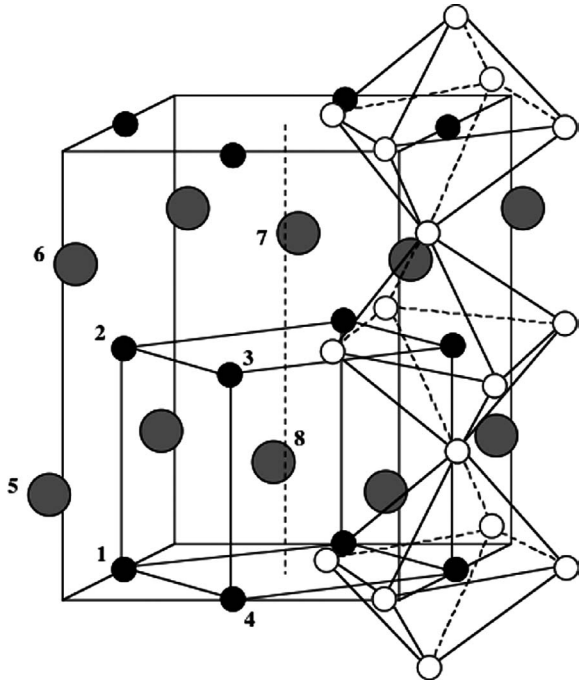

Fig. 4. Schematic structure of the $NdFe_{1-x}Co_xO_3$ unit cell. Fe and Co ions are depicted as black circles, Nd ions are larger grey circles. Both, Nd and the metals have been numbered as in Ref. [10]. The cube of the ideal perovskite as well as three distorted oxygen octahedra are shown.

tation, instead of the M, R subindices, capital letters are used for the M modes, while small ones refer to R modes.

In the particular case of $NdFe_{1-x}Co_xO_3$, R = Nd and M = Fe or Co, many experimental evidences [4,5] indicate that Co in $NdCoO_3$ is in a low-spin state and can be considered as a fully diamagnetic ion. Thus, it is possible to identify M = Fe in Eq. (1).

In $NdFeO_3$, below $T = 125$ K the Fe configuration is G_zF_x, belonging to the Γ_2 irreducible representation. As a consequence, the internal field $H_{\text{Fe–Nd}}$ produced by the Fe sublattice transforms as the Γ_2 irreducible representation, that in terms of the Nd allowed configuration modes corresponds to c_yf_x one [20]. Although the isotropic component of $H_{\text{Fe–Nd}}$ is compensated, the anisotropic one generates a noticeable polarization in the Nd system. Neutron diffraction experiments allowed to observe both the G_z mode of iron [21] and the c_y mode of Nd down to 1 K [22,6]. The ferromagnetic moments F_x of Fe and f_x of Nd are antiparallel and the spontaneous magnetization of the system becomes compensated at $T = 8$ K [23,24], but those modes have not been detected by neutron diffraction as they are very weak.

In previous works [2,6,7] we did develop a mean-field approximation for Nd orthoperovskites: Fe–Nd interaction was described by means of a staggered exchange field $H_{\text{Fe–Nd}}$ acting on the Nd system, while Nd–Nd interaction was described by a yet unknown mode belonging to another irreducible representation, as a true phase transition has been observed to take place at T_{N2}. At low temperatures, the $H_{\text{Fe–Nd}}$ field can be considered as independent of temperature, as Fe is fully saturated. On the Nd atom, we know that the first excited Kramers doublet is situated as high as 122 K above the ground doublet [25], which is the only doublet appreciably populated at the temperature range of this study. This allows us to use the effective spin 1/2 formalism. Indeed, the $\hat{\mathbf{s}}_{i,j}$ in Eq. (1) can be understood as spin 1/2 operators.

In Ref. [6], the model included the Van Vleck susceptibility of the Nd system, as it was needed to describe the temperature dependence of the neutron diffraction intensities in the paramagnetic region. However, as $\chi_{\text{V.V.}}$ has no influence on the specific heat calculation [6] it will not be taken into account in this work. Moreover, in order to reduce as much as possible the number of adjustable parameters, we will also neglect the presence of a f_x mode in the Nd configuration. There are two grounds for such a neglect. First, it has never been observed in neutron experiments (indicating that it is relatively weak). Second, to consider one or two allowed modes for Nd does not provide any thermodynamical difference into the model: the sizeable effect of $H_{\text{Fe–Nd}}$ transmitted into the calculated specific heat is to produce a Schottky effect through a Zeeman splitting which reduces the entropy available for cooperative ordering.

To a good approximation the effect of the $H_{\text{Fe–Nd}}$ internal field can be described by a Zeeman term with Bertaut's c_y (Γ_2) configuration. The Nd–Nd exchange interaction will be described, within a mean field model, by the following terms. The first one is proportional to the polarized mode, the c_y symmetry, which has as order parameter $\chi = -1/2 \cdot c_y^{®}$, as argued above. The second one corresponds to a cooperative mode, i.e., the mode which would appear in absence of the Fe sublattice. In a detailed neutron diffraction work on a single crystal of $NdFeO_3$ below T_{N2} [6] performed to determine the low-temperature configuration of the Nd sublattice, we concluded that the antiferromagnetic modes c_z (Γ_3) and c_x (Γ_1) could be excluded since the peaks that should appear in those case were not observed, and the ferromagnetic ones f_y (Γ_3) and f_z (Γ_4) were disregarded in this system (if present, these modes are small). We came to the conclusion that below T_{N2} only the non-centrosymmetric configurations Γ_5 (g_xa_y) and Γ_8 (a_xg_y) could appear in $NdFeO_3$, since these are the most often found in other orthoferrites [20], and also in $NdScO_3$ and $NdInO_3$ [3,26]. However, the $NdCoO_3$ has been found to order below $T_N = 1.20$ K in the c_z (Γ_1) configuration, so the presence of Co would tend to favour this configuration, when sufficient rate of substitution would be reached. In the low doses of substitution we are dealing with in this paper we adhere to either the Γ_5 or the Γ_8 configuration as the one present, in all likelihood, below T_{N2} in $NdFeO_3$. Since we observe a second order lambda peak at T_N there must be a lowering of symmetry in this transition, so below T_{N2} a new configuration must appear, superimposed to the c_y (Γ_2), which generates components perpendicular to the y axis, and not belonging to the c_z (Γ_1) configuration. We are left with the g_x (Γ_5) or a_x (Γ_8). Thus, the low-temperature configuration is $\Gamma_{2,5}$

S1293-2558(05)00072-5/FLA AID:2505 Vol.●●●(●●●)
SSSCIE:m5 v 1.36 Prn:8/04/2005; 12:11
ssscie2505
[DTD5] P.6 (1-10)
by:Vik p. 6

or $\Gamma_{2,8}$, corresponding to the modes $G_z F_x c_y g_x$ or $G_z F_x c_y a_x$ respectively. From the thermodynamic point of view, either choice gives the same results since the Hamiltonian is written in terms of a generic order parameter γ corresponding to $-\frac{1}{2}\langle\hat{\mathbf{g}}_x\rangle$ or $-\frac{1}{2}\langle\hat{\mathbf{a}}_x\rangle$, and we shall choose the former below.

The mean field Hamiltonian can be written in terms of these contribution, after due correction of the self-energy terms, following Ref. [27] procedure.

After subtraction of the appropriated self-interaction terms, the Hamiltonian for the Nd ions in a unit cell is:

$$H = -2\theta_c\gamma\hat{\mathbf{g}}_x - 2\theta_p\chi\hat{\mathbf{c}}_y + g_y\mu_B H_{\text{Fe-Nd}}\hat{\mathbf{c}}_y - 2\theta_c\gamma^2 - 2\theta_p\chi^2 \quad (2)$$

where the first and second terms describe the Nd–Nd exchange in cooperative and polarized modes, with exchange constants θ_c and θ_p, respectively. The mean-field order parameters for the cooperative and polarized modes are $\gamma = -\frac{1}{2}\langle\hat{\mathbf{g}}_x\rangle$ and $\chi = -\frac{1}{2}\langle\hat{\mathbf{c}}_y\rangle$. The third term is the Nd–Fe Zeeman term created by the $H_{\text{Fe-Nd}}$ exchange field. The two later terms are mean-field self-interaction corrections.

From this Hamiltonian, the free energy can be easily computed,

$$F = \frac{1}{2}\theta_c\gamma^2 + \frac{1}{2}\theta_p\chi^2 - T\ln\left[2\cosh\left(\frac{\Delta}{2T}\right)\right] \quad (3)$$

where

$$\Delta = \sqrt{(2\theta_c\gamma)^2 + (g_y\mu_B H_{\text{Fe-Nd}} + 2\theta_p\chi)^2} \quad (4)$$

is the exchange splitting of the Nd^{3+} ground doublet. By minimizing F with respect to γ and χ, one gets the characteristic equations:

$$\gamma = \gamma\frac{2\theta_c}{\Delta}\tanh\left(\frac{\Delta}{2T}\right), \quad (5)$$

$$\chi = \frac{(g_y\mu_B H_{\text{Fe-Nd}} + 2\theta_p\chi)}{\Delta}\tanh\left(\frac{\Delta}{2T}\right). \quad (6)$$

Two different solutions for Eq. (5) correspond to two distinct magnetic situations for the Nd system: the trivial $\gamma = 0$ corresponds to a polarized paramagnetic phase, and $\gamma \neq 0$ defines a polarized *and* cooperatively ordered phase. The intensity of the polarization of Nd by the $H_{\text{Fe-Nd}}$ internal field in $\hat{\mathbf{c}}_y$ mode (Γ_2 irreducible representation) is given at any temperature by χ.

The entropy of the Nd system can be calculated by derivation of Eq. (3);

$$S = \ln 2 + \ln\left[\cosh\left(\frac{\Delta}{2T}\right)\right] - \frac{\Delta}{2T}\tanh\left(\frac{\Delta}{2T}\right) \quad (7)$$

and the specific heat $C = T\delta S/\delta T$ can be easily computed numerically from this expression.

It is convenient to introduce the parameter $r = g_y\mu_B H_{\text{Fe-Nd}}/2(|\theta_p| - |\theta_c|)$, the ratio between the two types of exchange, Fe–Nd and Nd–Nd, since the predictions on the existence or inhibition of the long range transition may be expressed in terms of this adimensional parameter exclusively. The shape of the heat capacity curves calculated as a function of reduced temperature $t = 2k_B T/(|\theta_c| - |\theta_p|)$ for several r values are shown in Fig. 5. For $r = 0$, that is, in absence of any magnetic M (Fe) atom we obtain the molecular field prediction for the ordering of the Nd sublattice at T_{N2}. As r increases T_{N2} shifts to lower temperatures and decreases in height, while a Schottky contribution grows above the ordering temperature (upper panel of Fig. 5). For $r \geqslant 1$ the λ peak has disappeared, that is, the long range ordering is inhibited by the $H_{\text{Fe-Nd}}$ interaction (lower panel of Fig. 5). In Fig. 5, the $r = 0.95$ curve is shown in both panels to serve as a visual link between the $r < 1$ and $r > 1$ regimes. It is only in a narrow range of r values ($0.855 < r < 1$) that the Schottky anomaly shows a maximum at $T_{\max}$ while the Nd ordering λ peak is still visible. It is possible to emphasize this result by representing the ratio $T_{N2}/T_{\max}$ as a function of r as it is shown in Fig. 6. We also plot in this diagram the dots corresponding to actual $NdMO_3$ systems fitted by the model. Note the wide r range ($0 < r < 6$) taking place in isostructural $NdMO_3$ compounds.

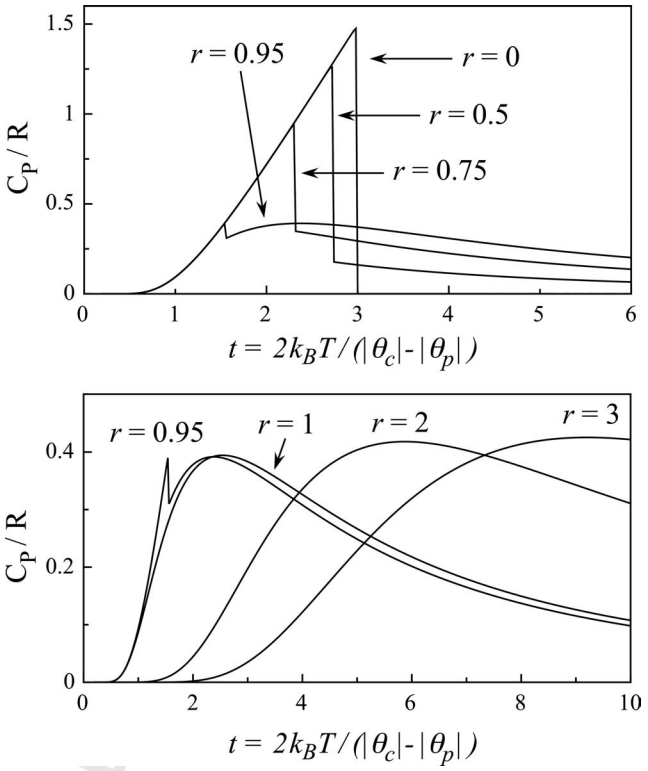

Fig. 5. Specific heat curves as a function of reduced temperature $t = 2k_B T/(|\theta_c| - |\theta_p|)$ for different values of r calculated with the mean field model described in this work. In the top panel, curves with $r < 1$ are shown, while in the lower panel, curves with $r \geqslant 1$ curves are compared with the $r = 0.95$ one.

In Fig. 5 we show the specific heat curves for different values of r calculated with the mean field model described in this work. In the top panel, several curves with $r < 1$ are shown. The variation from the classical mean field model result for an isolated lattice ($r = 0$) evolves towards a

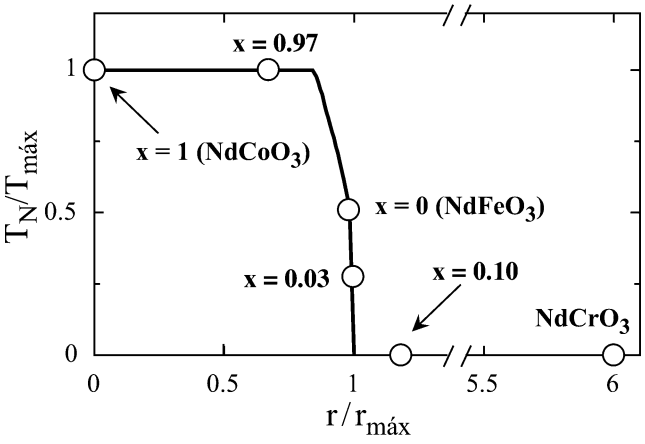

Fig. 6. The T_{N2}/T_{max} ratio is shown as a function of r. The values corresponding to several $NdMO_3$ systems fitted by the model are also shown.

Schottky-like specific heat. In the lower panel, $r \geqslant 1$ curves are compared with the $r = 0.95$ one. For high r values (as the Nd–Nd interaction becomes lower than the Fe–Nd one) the specific heat curve tends to a pure 2-level Schottky curve.

Our heat capacity results for $x = 0$ are satisfactorily fitted with the parameter values $\theta_c = 2.7$ K and $\theta_p = -0.83$ K, equivalent to an average exchange interaction of $J/k_B = -0.88$ K between Nd ions, and $r = 0.979$, that is, a net internal field of $H_{Fe-Nd} = 59$ kOe, taken into account that in $NdFeO_3$ $\mu_{Nd} = 0.92\mu_B$ [6].

The introduction of magnetic vacancies as a random substitution of Fe atoms lets each Nd atom loose one or more magnetic nearest neighbour Fe atom (see Fig. 7). The net effect is a further decompensation of the internal field due to a contribution from the isotropic and anisotropic components of the Fe–Nd interaction. We propose that the vacancies do not modify the symmetry of the Fe sublattice, or that this is a negligible effect. Thus, the contribution due to the uncompensated Fe moment is assumed to conform to the same Fe sublattice symmetry and, therefore, with the same Nd configuration as the $x = 0$ mean H_{Fe-Nd}, i.e., the c_y configuration.

Since the substitution is random, the internal field due to one vacancy in a pseudocubic cell, comprising $z = 8$

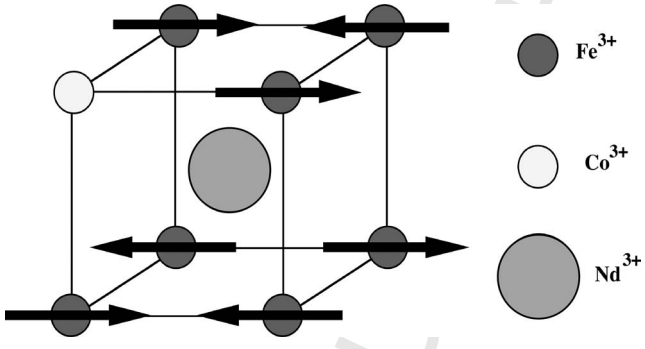

Fig. 7. Schematic representation of the first neighbours of a particular Nd ion in $NdFe_{1-x}Co_xO_3$ ($x > 0$). A diamagnetic Co atom (○) has substituted a Fe site (●), generating a magnetic vacancy.

Fe moments acting on a Nd moment, can be written as $H_{Fe-Nd} = \eta H_{ex} c_y$, with $\eta = \pm 1$, depending on which type of position is occupied by the magnetic vacancy. Hence, it can add or subtract to the anisotropic average field H_{Fe-Nd} [12]. Besides, H_{Fe-Nd} will also be reduced due to the loss of one compensated pair of contributing Fe spins. Therefore the effective field acting on the Nd moment is

$$H_{eff} = \frac{z-2}{z} H_{Fe-Nd} + \eta H_{ex} c_y. \tag{8}$$

We only need to substitute H_{Fe-Nd} by H_{eff} in Δ (Eq. (4)) to obtain the perturbed splitting energy. Two values of the perturbed splitting arise, $\Delta^{\pm}$, corresponding respectively to the values $\eta = \pm 1$. We note that H_{eff} enters into a binomial in Eq. (4) and this shifts the center of gravity of the doublet respect to Δ. The free energy of the system has to be modified consequently with three terms weighted by the number of Nd ions unperturbed and perturbed by the fraction x of vacancies:

$$F = \frac{1}{2}\theta_c \gamma^2 + \frac{1}{2}\theta_p \chi^2 - (1-zx)T \ln\left[2\cosh\left(\frac{\Delta}{2T}\right)\right] + \frac{1}{2}\sum_{\eta=\pm 1} zxT \ln\left[2\cosh\left(\frac{\Delta}{2T}\right)\right]. \tag{9}$$

Minimizing this expression respect to γ and χ, the order parameter evolution with temperature can be numerically computed, and the heat capacity thereafter. The net result is equivalent to having a perturbing field superposed to the average H_{Fe-Nd}, which is the value deduced from experiment.

Depending on the substitution rate the number of uncompensated spins varies. The fit to the $x = 0.03$ heat capacity curve, as shown in Fig. 8, is achieved with the same θ and θ_2 parameters as for the pure compound but with $r = 0.995$, or equivalently $H_{Fe-Nd} = 60$ kOe, that is, a 1.5% increase. This value of r is in the range where both the Schottky maximum and the lambda peak are still observable. However, for $x = 0.1$ the lambda peak has disappeared completely while the Schottky anomaly is well developed. As seen in Fig. 8 the latter is shifted to higher temperature in comparison to the $x = 0$ curve, indicating a larger splitting of the Nd ground doublet. In this case $r = 1.18$, beyond the limit of inhibition of the long range ordering Nd sublattice transition, implying an average internal field $H_{Fe-Nd} = 71$ kOe. A detailed plot of the experimental and theoretical results for the temperature range around $T \sim 1$ K for $x = 0$, 0.03 and 0.1 is shown in Fig. 9. There, the inhibition of Nd magnetic order with increasing Co concentration can be clearly observed. Note that Fig. 6 includes the dots corresponding to these three concentration.

For $x > 0$ the Schottky part of the heat capacity curves is broader and stands lower than just one Schottky anomaly. The substitution of Fe by magnetic vacancies produces a distribution of exchange fields that cannot be mimicked by just an average field. To describe the distribution of Nd ions having decompensated nearest neighbouring Fe spins we introduce the parameter G. At a given Nd site, $G = 0$ indicates

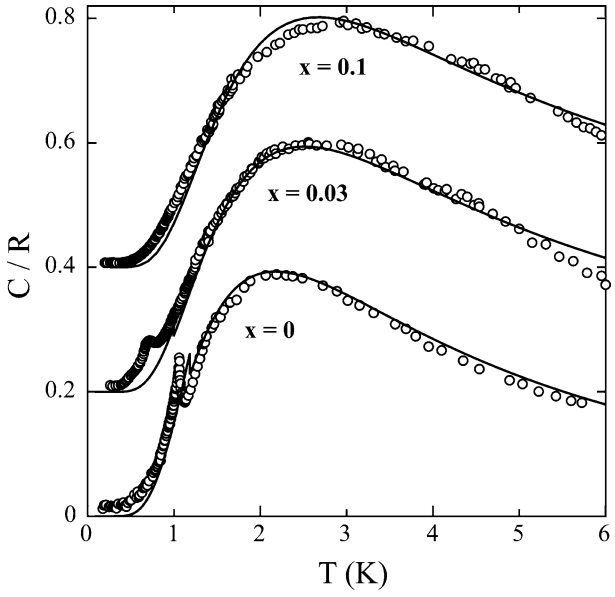

Fig. 8. Experimental specific heat for $NdFe_{1-x}Co_xO_3$ with $x = 0$, 0.03 and 0.1 compared to the results of the main field model as detailed in the text.

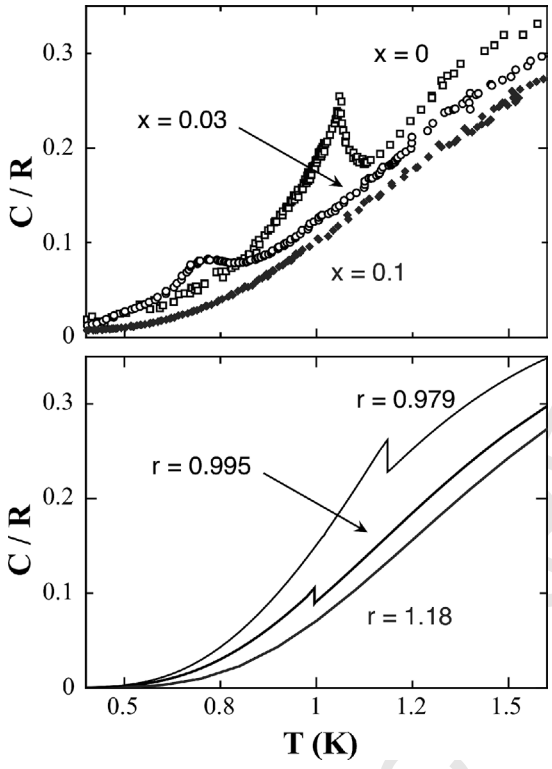

Fig. 9. A detail of the experimental (upper panel) specific heat for $x = 0$ (open squares), 0.03 (black circles) and 0.1 (grey diamonds) and the corresponding calculated curves (lower panel) with the indicated r values, around T_{N2}.

the presence of an equal number of surrounding Fe spins in one direction than in the opposite (varying from 4 for no vacancies around the Nd to 0 for no Fe atoms), $G = 1$ corresponds to a situation with one spin in excess in a direction than in the opposite, $G = 2$ corresponds to two uncompensated spins, and so on. We have calculated the fraction of Nd ions with a given G value for a fixed Co concentration. The results are given in Table 2. For $x = 0.03$ nearly 20% of the Nd have decompensation by one spin ($G = 1$) and only 1% by two ($G = 2$). For $x = 0.1$ only 52% retain a compensated environment, 41% have $G = 1$ and 6.6% are decompensated by two spins ($G = 2$). Since the substitution is random (or expected to be so) the net effect could be expected to cancel out. However, what we observe is equivalent to an increase in the average $H_{Fe–Nd}$ interaction.

Table 2
Fraction p_G of Nd^{3+} ions with a degree G of antiferromagnetic uncompensation defined in the text as a function of the Co concentration in $NdFe_{1-x}Co_xO_3$. Values of the order of 10^{-4} or less are indicated as ∼0

G	$x = 0$	$x = 0.03$	$x = 0.1$	$x = 0.25$	$x = 0.5$
0	1	0.796	0.518	0.325	0.274
1	0	0.195	0.411	0.465	0.437
2	0	0.009	0.066	0.175	0.219
3	0	∼0	0.005	0.033	0.062
4	0	∼0	∼0	0.002	0.008

Since the Schottky heat capacity depends just on one parameter, the doublet splitting, and it is a single particle contribution without cooperative effects, it can be calculated as a weighted sum of contributions with $G = 0$ to 4:

$$C_p = \sum_{G=0}^{4} p_G \,\mathrm{Sch}(\Delta_G) \tag{10}$$

where the weight p_G are given in Table 2 and the function $\mathrm{Sch}(\Delta_G)$ is the Schottky specific heat for a two-level system with splitting Δ_G. The $x = 0.03$, 0.1, 0.25, and 0.5 curves have been fitted under this hypothesis to account for the broadening effect on the Schottky anomaly, disregarding the lambda anomaly in $x = 0.03$. In practice, as the p_3 and p_4 fractions are always very small and its effects (if any) appear at high temperatures, we have minimized the number of terms in Eq. (10) used in the fits. The curves are very well fitted, as can be checked by inspection of Fig. 10. The total set of results are given in Table 3. The p_G and Δ_G values obtained from the fits allow us to obtain the weighted averaged Δ_{Schott} as shown in the inset of Fig. 2. Notwithstanding the excellent fits, we note that for $x = 0.5$ the fit is not as good. Although a less precise determination of the non-magnetic base-line (since it has a larger part at higher temperatures) cannot be fully ruled out, the quality of the fit is probably

Table 3
Energy splittings Δ_G of the Nd^{3+} ground doublet as obtained from the fit of the experimental curves shown in Fig. 10 according to Eq. (10)

E/k_B (K)	$x = 0.03$	$x = 0.1$	$x = 0.25$	$x = 0.5$
Δ_0	5.31(1)	4.93(6)	4.05(4)	3.32(3)
Δ_1	10.4(1)	8.15(7)	7.65(5)	7.19(4)
Δ_2		12.1(5)	10.2(3)	15.6(2)
Δ_3				34.6(1.2)

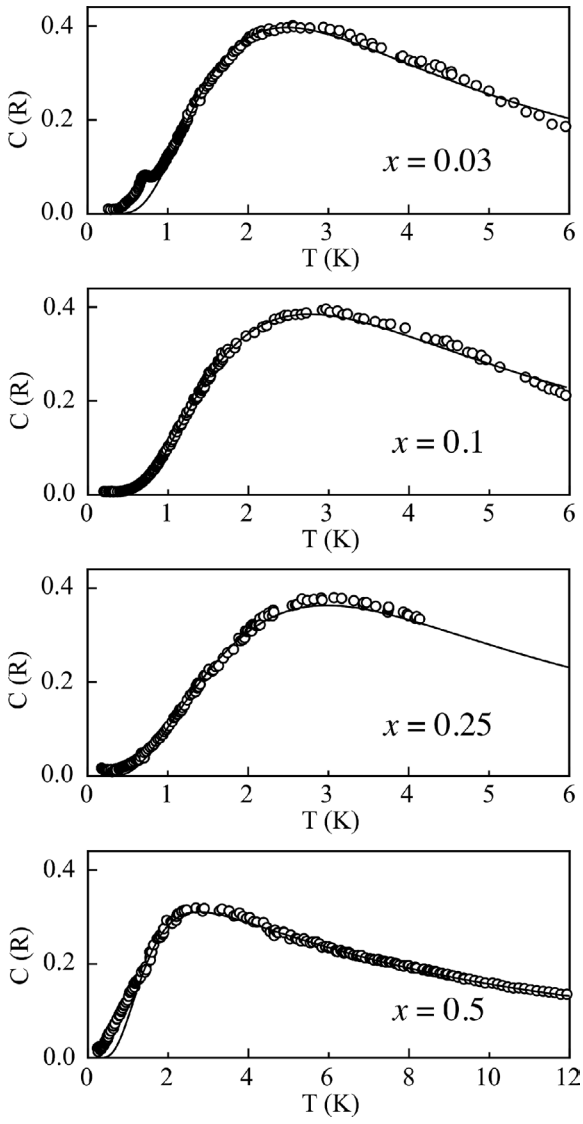

Fig. 10. Comparison between the experimental specific heat of $NdFe_{1-x}Co_xO_3$ for $x = 0.03$, 0.1, 0.25 and 0.5 and the calculated curves after Eq. (10) with the values given in Tables 2 and 3.

more affected by the limitation of the number of Δ_G to 5. Obviously, the splitting caused in the Nd^{3+} ground doublet by the different arrangements leading to a given G value are not necessarily equal, as Eq. (10) implies, but it is taken as a compromise to minimize the number of free parameters.

5. Discussion

The evolution of the $NdFeO_3$ heat capacity upon substitution of Fe by non-magnetic Co, that is for $0 \leqslant x \leqslant 0.5$ needs to consider that the Fe sublattice retain long range ordering in spite of the magnetic dilution of the Fe sublattice. Using Mössbauer spectroscopy in $LaFe_{1-x}Co_xO_3$ [28], the Fe sublattice is found to be well ordered at room temperature for $x < 0.5$. The nearest neighbors to a Nd^{3+} ion are eight Fe^{3+} moments antiferromagnetically coupled in the Γ_2 configuration.

For $x = 0$ the effective field should be nearly compensated by symmetry. As we proved earlier [6] the compensation is not complete, though, and a mean staggered field $H_{\mathrm{Nd-Fe}}$ acts on the Nd moment. As a result the Nd^{3+} ground state doublet splits; then the Nd moments are polarized in a Γ_2 configuration giving rise to a Schottky anomaly. As the Nd–Nd interaction becomes of the order of k_BT, a long range magnetic ordering of the Nd sublattice to the $\Gamma_{R,2}$ ($R = 5, 8$) configuration takes place at T_{N2}.

As a result of the introduction of magnetic vacancies on the system, an uncompensated isotropic exchange field acts on the rare earth ion with the same antiferromagnetic mode as the Fe sublattice, but factorized locally by a number given by the uncompensated spins. Therefore two types of fields will act on the rare earth ion, a regular field as in the pure compound, and a random field produced by the vacancies. Besides, the Nd–Nd interaction is assumed to be not affected by the Co substitution.

As we have shown in the experimental section, the net effect in $NdFe_{1-x}Co_xO_3$, $0 \leqslant x \leqslant 0.03$, is to increase the average field $H_{\mathrm{Nd-Fe}}$ which splits the Nd^{3+} ground state and competes with the $H_{\mathrm{Nd-Nd}}$ in the Γ_2 to $\Gamma_{R,2}$ (with $R = 5$ or 8) transition at T_{N2}, shifting the transition to lower temperatures up to its quenching for $x = 0.1$. The model developed in Section 4 explains quantitatively all these features and allows to determine the rate of decrease in temperature versus substitution $\Delta T/\Delta x = 6.6$ K/atom.

In the substituted compounds, the Schottky anomaly cannot be explained in terms of an exchange field only, however it is well fitted by a weighted sum of 2, 3 or 4 Schottky anomalies, for $x = 0.03$, 0.1, 0.25, and $x = 0.5$, respectively. Table 3 indicates the deduced weights and splittings. The fields are different because of the different ways that the uncompensation is produced by the vacancies, and the weight are calculated as the probability to have $G = 0$, 1, 2, 3 or 4 uncompensated moments. The excellent fit obtained with this simple model confirms the initial proposition that each vacancy contributes by an approximately constant amount to the internal field acting on the Nd^{3+} ion. Indeed, the internal field increases by a nearly constant proportion per decompensation unit of G, except for $x = 0.5$, where the fits are probably oversimplified as seen on Table 3. Besides, it can be appreciated from this Table 3 that the value of Δ_0 decreases with increasing substitution. It is probable that the anisotropic average field is lower for lower number of compensated pairs of n.n. neighbors, under the conjecture that each pair of compensated spins gives a contribution to $H_{\mathrm{Fe-Nd}}$. Since for $x > 0$ the value Δ_0 is averaged over the 4–4, 3–3, 2–2, 1–1 and 0–0 combinations with a common $G = 0$ parameter, therefore for increasing x there is an increasing weight of the highly-substituted configurations in this trend of $G = 0$ combinations. As a result, the average Δ_0 lowers its value.

6. Conclusions

We have proven that in the case of substitution of Fe atoms by Co in $NdFeO_3$, equivalent to the inclusion of magnetic vacancies at the Fe sites, the Nd atoms are polarized by an effective field originating from the Fe sublattice. This field increases in intensity if the number of vacancies increases. The Nd sublattice undergoes a second order transition from the polarized state, c_y (Γ_2), to a polarized and long range ordered configuration of lower symmetry, $c_y g_x$ ($\Gamma_{2,5}$) or $c_y a_x$ ($\Gamma_{2,8}$), if the rate of substitution does not exceed $x = 0.05$. Indeed, from the increasing number of vacancies results an increase in the $H_{\text{Fe–Nd}}$ filed which overcomes the Nd–Nd interaction and inhibits the long range order transition. This effect due to vacancies is different to that induced in other orthoferrites, where spin reorientation transitions increase in temperature, decrease, or even are induced. On the other hand, it is similar to the inhibition by vacancies of the Tb long range ordering in $TbFe_{1-x}Al_xO_3$, although in the Tb case, a rate of substitution of $x = 0.025$ already reveals effective [13].

Acknowledgements

The authors are indebted to Professor E.F. Bertaut, for his human and scientific insight and inspiration, and in particular for actively contributing to the development of the solid state physics at Zaragoza during the last decades as the former Director of the *Laboratoire de Cristallographie* of the CNRS at Grenoble.

This work has been financed by the Fundación Areces, CICYT MAT02-04178-C04, MAT02-0166 and DGA-P04/2001 projects.

References

[1] F. Bartolomé, M. Kuz'min, R. Merino, J. Bartolomé, IEEE Trans. Magn. 30 (1994) 960.
[2] F. Bartolomé, M. Kuz'min, J. Bartolomé, J. Blasco, J. García, F. Sapiña, Solid State Commun. 91 (1994) 177.
[3] J. Bartolomé, F. Bartolomé, Phase Trans. 64 (1997) 57.
[4] J.B. Goodenough, J.M. Longo, Landolt-Börnstein New Series, vol. III/4a, Springer-Verlag, New York, 1970.
[5] H.P.J. Wijn, Landolt-Börnstein New Series, vol. III27/f3, Springer-Verlag, New York, 1994.
[6] J. Bartolomé, E. Palacios, M.D. Kuz'min, F. Bartolomé, I. Sosnowska, R. Przenioslo, R. Sonntag, M.M. Lukina, Phys. Rev. B 55 (1997) 11432.
[7] F. Bartolomé, J. Bartolomé, R. Eccleston, J. Appl. Phys. 87 (2000) 7052.
[8] F. Bartolomé, J. Bartolomé, M. Castro, J. Melero, Phys. Rev. B 62 (2000) 1058.
[9] F. Bartolomé, 2004, in press.
[10] E. Bertaut, in: G.T. Rado, H. Suhl (Eds.), Magnetism, vol. III, Academic Press, New York and London, 1963, p. 86.
[11] P. Pataud, J. Sivardière, J. Phys. (Fr) 31 (1970) 1017.
[12] A.M. Kadomtseva, A.K. Zvezdin, M.M. Lukina, V.N. Milov, A.A. Mukhin, T.L. Ovchinnikova, Sov. Phys. JETP 46 (1977) 1216.
[13] V.N. Derkachenko, A.K. Zvezdin, A.M. Kadomtseva, N. Kovtun, M.M. Lukina, A.A. Mukhin, Phys. Stat. Sol. (a) 84 (1984) 215.
[14] A.K. Zvezdin, A.M. Kadomtseva, A.A. Mukhin, Izv. Akad. Nauk SSSR Ser. Fiz. 44 (1980) 1348.
[15] G.P. Vorob'ev, A.M. Kadomtseva, I.B. Krynetskii, M.M. Lukina, A.A. Mukhin, Sov. Phys. JETP 72 (1991) 736.
[16] W.C. Koehler, E.O. Wollan, M.K. Wilkinson, Phys. Rev. 58 (1960) 118.
[17] F. Luis, M.D. Kuz'min, F. Bartolomé, V.M. Orera, J. Bartolomé, M. Artigas, J. Rubín, Phys. Rev. B 58 (1998) 798.
[18] V.K.S. Shante, S. Kirkpatrick, Adv. Phys. 20 (1973) 235.
[19] E. Palacios, J. Bartolomé, F. Luis, R. Sonntag, Phys. Rev. B 68 (2003) 224425.
[20] K.P. Belov, A.K. Zvezdin, A.M. Kadomtseva, in: Rare-Earth Orthoferrites, Symmetry and Non-Heisenberg Exchange, in: Sov. Sci. Rev. A, vol. 9, Harwood Academic Publishers, New York, 1987, p. 117.
[21] P. Pataud, J. Sivardière, J. Phys. (Fr) 31 (1970) 803.
[22] I. Sosnowska, P. Fischer, Phase Trans. 8 (1987) 319.
[23] K.P. Belov, M.A. Belkyanchikova, A.M. Kadomtseva, I.B. Krynetskii, T.M. Ledneva, T.L. Ovchinnikova, V.A. Timofeeva, Sov. Phys. Solid State 14 (1972) 199.
[24] R.M. Hornreich, I. Yaeger, Int. J. Magn. 4 (1973) 71.
[25] M. Loewenhaupt, I. Sosnowska, B. Frick, J. Phys. (Fr) C8-921 (1988) 803.
[26] I. Plaza, E. Palacios, J. Bartolomé, S. Rosenkranz, C. Ritter, A. Furrer, Physica B 234–236 (1997) 632.
[27] B. Diu, Physique Statistique, Hermann, Paris, 1989.
[28] Y.Q. Jia, S.T. Liu, Y. Wu, M.Z. Jin, X.W. Liu, M.L. Liu, Phys. Stat. Sol. A 143 (1994) 15.